Journal of Pathology
J Pathol February 2021; **253:** 234–245
Published online 4 December 2020 in Wiley Online Library (wileyonlinelibrary.com) DOI: 10.1002/path.5584

ORIGINAL PAPER

CDKN1B mutation and copy number variation are associated with tumor aggressiveness in luminal breast cancer

Davide Viotto[1†], Francesca Russo[1,2†], Ilaria Anania[1], Ilenia Segatto[1], Gian Luca Rampioni Vinciguerra[1,3], Alessandra Dall'Acqua[1], Riccardo Bomben[4], Tiziana Perin[5], Martina Cusan[1], Monica Schiappacassi[1], Lorenzo Gerratana[6,7], Sara D'Andrea[1], Francesca Citron[1], Filippo Vit[2,4], Lorena Musco[1,2], Maria Chiara Mattevi[1], Giorgia Mungo[1], Milena S Nicoloso[1,6], Maura Sonego[1], Samuele Massarut[8], Roberto Sorio[6], Luigi Barzan[9], Giovanni Franchin[10], Giorgio Giorda[11], Emilio Lucia[11], Sandro Sulfaro[12], Vittorio Giacomarra[9], Jerry Polesel[13], Federica Toffolutti[13], Vincenzo Canzonieri[5,14], Fabio Puglisi[6,7], Valter Gattei[4], Andrea Vecchione[3], Barbara Belletti[1‡*] and Gustavo Baldassarre[1‡]

[1] *Molecular Oncology Unit, Centro di Riferimento Oncologico di Aviano (CRO Aviano), IRCCS, National Cancer Institute, Aviano, Italy*
[2] *University of Trieste, Trieste, Italy*
[3] *Department of Clinical and Molecular Medicine, University of Rome 'Sapienza', Sant'Andrea Hospital, Rome, Italy*
[4] *Onco-Hematology Unit, Centro di Riferimento Oncologico di Aviano (CRO Aviano), IRCCS, National Cancer Institute, Aviano, Italy*
[5] *Pathology Unit, Centro di Riferimento Oncologico di Aviano (CRO Aviano), IRCCS, National Cancer Institute, Aviano, Italy*
[6] *Department of Medical Oncology, Centro di Riferimento Oncologico di Aviano (CRO Aviano), IRCCS, National Cancer Institute, Aviano, Italy*
[7] *Department of Medicine (DAME), University of Udine, Udine, Italy*
[8] *Breast Surgery Unit, Centro di Riferimento Oncologico di Aviano (CRO Aviano), IRCCS, National Cancer Institute, Aviano, Italy*
[9] *Division of Otorhinolaryngology, General Hospital of Pordenone Santa Maria degli Angeli, Pordenone, Italy*
[10] *Radiotherapy Unit, Centro di Riferimento Oncologico di Aviano (CRO Aviano), IRCCS, National Cancer Institute, Aviano, Italy*
[11] *Gynecological Surgery Unit, Centro di Riferimento Oncologico di Aviano (CRO Aviano), IRCCS, National Cancer Institute, Aviano, Italy*
[12] *Unit of Pathology, General Hospital of Pordenone Santa Maria degli Angeli, Pordenone, Italy*
[13] *Cancer Epidemiology Unit, Centro di Riferimento Oncologico di Aviano (CRO Aviano), IRCCS, National Cancer Institute, Aviano, Italy*
[14] *Department of Medical, Surgical and Health Sciences, University of Trieste, Trieste, Italy*

**Correspondence to: B Belletti, Centro di Riferimento Oncologico di Aviano (CRO Aviano), IRCCS, National Cancer Institute, Via Gallini 2, 33170 Aviano, Italy. E-mail: bbelletti@cro.it*

[†]Equal contributions
[‡]B Belletti and G Baldassarre share last co-authorship.

Abstract

The *CDKN1B* gene, encoding for the CDK inhibitor p27[kip1], is mutated in defined human cancer subtypes, including breast, prostate carcinomas and small intestine neuroendocrine tumors. Lessons learned from small intestine neuroendocrine tumors suggest that *CDKN1B* mutations could be subclonal, raising the question of whether a deeper sequencing approach could lead to the identification of higher numbers of patients with mutations. Here, we addressed this question and analyzed human cancer biopsies from breast (*n* = 396), ovarian (*n* = 110) and head and neck squamous carcinoma (*n* = 202) patients, using an ultra-deep sequencing approach. Notwithstanding this effort, the mutation rate of *CDKN1B* remained substantially aligned with values from the literature, showing that essentially only hormone receptor-positive breast cancer displayed *CDKN1B* mutations in a relevant number of cases (3%). However, the analysis of copy number variation showed that another fraction of luminal breast cancer displayed loss (8%) or gain (6%) of the *CDKN1B* gene, further reinforcing the idea that the function of p27[kip1] is important in this type of tumor. Intriguingly, an enrichment for *CDKN1B* alterations was found in samples from premenopausal luminal breast cancer patients (*n* = 227, 4%) and in circulating cell-free DNA from metastatic luminal breast cancer patients (*n* = 59, 8.5%), suggesting that *CDKN1B* alterations could correlate with tumor aggressiveness and/or occur later during disease progression. Notably, many of the identified somatic mutations resulted in p27[kip1] protein truncation, leading to loss of most of the protein or of its C-terminal domain. Using a gene-editing approach in a luminal breast cancer cell line, MCF-7, we observed that the expression of p27[kip1] truncating mutants that lose the C-terminal domains failed to rescue most of the phenotypes induced by *CDKN1B* gene knockout, indicating that the functions retained by the C-terminal portion are critical for its role as an oncosuppressor, at least in luminal breast cancer.

Keywords: *CDKN1B*; p27; mutation; copy number variation, CNV; breast cancer; young breast cancer patients; liquid biopsy; ovarian cancer; head and neck squamous cell carcinoma

Received 22 May 2020; Revised 12 October 2020; Accepted 29 October 2020

No conflicts of interest were declared.

Introduction

The tumor suppressor gene *CDKN1B*, encoding the cell cycle inhibitor $p27^{kip1}$ (hereafter p27), is rarely mutated in cancer. So far, it has been found to be mutated in only a few types of tumor, such as prostate cancer [1] and small intestine neuroendocrine tumors (SI-NETs), a rare malignant neoplasm arising from neuroendocrine precursor cells, in which *CDKN1B* represents the most frequently mutated gene [2]. *CDKN1B* germline mutations have been proposed to be the cause of multiple endocrine neoplasia type 4 (MEN4), an autosomal dominant disorder, characterized by the occurrence of tumors in endocrine glands [3]. These data not only confirmed that *CDKN1B* is a *bona fide* tumor suppressor gene in humans, as widely demonstrated in mice [4,5], but also suggested that p27 deregulation is particularly involved in endocrine neoplasia, and more generally in human cancers that rely on or respond to hormones.

Next generation sequence (NGS) analyses have redefined the molecular classification of breast cancer; many new potential drivers of tumor progression have been identified [6–9]. These mutations are in part common to the different breast cancer subtypes and in part specific for each subtype. Sometimes, mutated driver genes are in the root cancer clone, whereas on other occasions the presence of multiple drivers is associated with subclonal evolution of the cancer [6–9]. Among the latter, *CDKN1B* was identified as a driver gene, almost exclusively mutated in luminal breast cancer (LBC) [6–11]. It is worth noting that most of the *CDKN1B* mutations described in cancer (LBC, SI-NET and prostate cancer) are nonsense and/or small deletions/insertions that cause the production of a truncated protein that sometimes retains the cyclin-CDK binding domain, but almost invariably loses the C-terminus [12]. A very recent work has also highlighted that alterations leading to loss of function of *CDKN1B* are enriched in metastatic samples from breast cancer patients [13].

Interestingly, expression and functional studies have demonstrated that high p27 expression predicts sensitivity to endocrine and chemotherapy in LBC patients [14,15], whereas p27 downregulation predicts resistance to radiotherapy [16] and anti-HER2 therapies [17–19]. The role of p27 in LBC has recently acquired further translational relevance as new crystal structural data have demonstrated that p27 can prevent CDK4/6 inhibitors (e.g. palbociclib) from binding and inhibiting their targets, CDK4/6. This mechanism would eventually lead to resistance to these small molecule inhibitors, which have been recently approved for the treatment of LBC, showing very promising results [20,21].

The study of SI-NETs demonstrated that *CDKN1B* mutations could be subclonal and that the use of a deeper NGS approach allowed the finding of a number of mutated samples higher than the ones retrieved by a whole-exome sequencing approach, based on low coverage [2]. Here, we tested if the same observation could be made in other tumor types, using breast, head and neck and ovarian cancer as study models.

Materials and methods

Ethical statement

Solid tumor specimens from breast, ovarian and head and neck cancer patients and liquid biopsies from metastatic breast cancer patients were collected after signed written informed consent was obtained, in accordance with recognized ethical guidelines and following approval by the Institutional Review Board of CRO Aviano, National Cancer Institute (Aviano, Italy) and University of Rome 'Sapienza' Sant'Andrea Hospital (Rome, Italy). All studies were performed in compliance with the 1975 Declaration of Helsinki, as revised in 1983.

Primary tumor collection

Human breast cancer specimens collected at CRO Aviano were taken by the pathologist directly after surgery and immediately frozen, or flash frozen in OCT compound, as more appropriate in each circumstance, and stored in the institutional biobank until needed. Human breast cancer specimens collected at University of Rome 'Sapienza', were fixed in 4% buffered (pH 7.4) formaldehyde and stored until needed. Histological re-evaluation of tumor representative sections was performed by the Pathology Units of CRO Aviano and University of Rome 'Sapienza'. Tumor stage was assessed according to the American Joint Committee on Cancer (8th edition) [22]. Expression of hormone receptors (ER clone SP1, cat. # 790-4324, pre-diluted; PgR clone 1E2, cat. # 790-4296, pre-diluted; Ventana, Roche, Basel, Switzerland), HER2 (HER2 clone 4B5, cat. # 790-2991, pre-diluted; Ventana) and proliferation index (Ki-67, clone 30-9, cat. # 790-4286, pre-diluted; Ventana) were evaluated by immunohistochemistry (Ultraview Detection Kit cat. #760-500; Ventana); HER2 status was measured and reported according to ASCO-CAP 2018 guidelines [23]. Then, breast tumors were classified in accordance with WHO 2019 [24].

Human epithelial ovarian cancer specimens were collected at surgery by the pathologist at CRO Aviano, immediately frozen and stored in the institutional biobank until needed. Histological re-evaluation of tumor representative sections from surgical specimens was performed by the Pathology Unit of CRO Aviano and tumor stage was assessed according to WHO 2017 [25].

Specimens from primary head and neck squamous cell carcinomas (HNSCC) were collected from patients who underwent surgery at CRO Aviano and General Hospital of Pordenone, immediately frozen and stored in the CRO institutional biobank until needed. Pathological evaluation of tumor biopsies was made by the Pathology Unit of General Hospital of Pordenone. Tumor stage (cT/cN) was clinically assessed according to the American Joint Committee on Cancer (8th edition) [22].

DNA purification, NGS analyses and droplet digital PCR

The Maxwell® 16 Tissue DNA Purification Kit (Promega, Madison, WI, USA) was used for automated purification of DNA from fresh solid tumor samples, following the manufacturer's instructions. The AllPrep DNA/RNA mini kit and AllPrep DNA/RNA FFPE kit (Qiagen, Hilden, Germany) were used for manual purification of DNA from cryosections or formalin-fixed paraffin-embedded (FFPE) sections from solid tumor samples, respectively, following the manufacturer's instructions. The Maxwell® RSC ccfDNA plasma kit (Promega) was used for automated purification of circulating cell-free DNA (ccfDNA) from plasma of metastatic LBC patients. Plasma was obtained by centrifuging whole blood from EDTA tubes 1× for 10 min at 2000 × *g* and 2× for 10 min at 4000 × *g*. DNA quantification was performed using the QuantiFluor® ONE dsDNA System (Promega).

Details for DNA purification, amplification, droplet digital PCR (ddPCR) and NGS can be found in Supplementary materials and methods.

Bioinformatic analysis

CDKN1B somatic mutations of possible clinical significance were evaluated by curated analyses of Catalogue of Somatic Mutations in Cancer (COSMIC, https://cancer.sanger.ac.uk/cosmic) and International Cancer Genome Consortium (ICGC, https://dcc.icgc.org/) data portals.

NGS data were mapped to the human reference genome (GRCh37/hg19, https://www.ncbi.nlm.nih.gov/assembly/GCF_000001405.13/, accessed September 2020) Data were analyzed with VariantStudio™ software (Illumina, San Diego, CA, USA) and Integrative Genomics Viewer software [26]. After quality check controls and filtering, reads and variants distributed in target regions were analyzed and annotated. Results were expressed as a percentage of mutated DNA. Only somatic alterations called at allele frequencies ≥1% and that were confirmed in at least two distinct runs were considered mutated. Synonymous variants and polymorphisms described in the Single Nucleotide Polymorphism Database (dbSNP138) [27] were removed.

Cell culture and *in vitro* assays

MCF-7 and T47D LBC cell lines were obtained from ATCC (LGC Standards, Manassas, VA, USA) and grown in DMEM (Merck Life Science, Darmstadt, Germany) supplemented with 10% FBS (Carlo Erba, Milano, Italy), at standard conditions of 37 °C and 5% CO_2. The generation of MCF-7 p27 knockout (KO) cell clones was as described previously [28]. Based on two *CDKN1B* truncating mutations discovered by Ellis *et al* [8], p27 K134fs and p27 T171*, we generated mutant p27 knockin (KI) cell clones, as described in Supplementary materials and methods.

T47D, MCF-7 parental cell line and descendent KO and KI clones were authenticated by STR analysis, according to the PowerPlex® 16 HS System (Promega) protocol and using GeneMapper™ software 5 (Thermo Fisher Scientific, Waltham, MA, USA) to identify DNA STR profiles. All cell lines were routinely tested to exclude Mycoplasma contamination (MycoAlert™, Lonza, Basel, Switzerland).

Growth curves, cell cycle distribution by fluorescence-activated cell sorting (FACS) analysis, anchorage-independent cell growth and three-dimensional (3D) mammary epithelial cell growth were determined as described previously [29–33]. Multiple cell clones were always tested in each assay, in duplicates or triplicates as appropriate.

Immunofluorescence, western blotting, immunoprecipitation and kinase assays

All analyses were performed as described previously [28–30,32,33] and are described in detail in supplementary material, Supplementary materials and methods. For the analysis of protein stability, cycloheximide (Merck Life Science) was added to cell culture medium at 10 μg/ml and cells were collected at the indicated times and processed to prepare protein lysates for western blot analyses.

RT-qPCR

Total RNA was extracted in TRIzol reagent following the manufacturer's instructions (Invitrogen, Thermo Fisher Scientific). RNA purification, quantification and RT-qPCR were performed as described previously [29,32]. All methods and the primers used are described in detail in Supplementary materials and methods.

Statistical analyses

Statistical significance, mean, median and SD were determined using PRISM software (version 6.01) (GraphPad Inc., San Diego, CA, USA), using the most appropriate test, as specified in each figure. A minimum of three biologically independent experiments was used for statistical significance. The number and type of replicates used in each experiment are specified in the figure legends. When not otherwise specified, mean and SD are shown in all graphs. Significance was calculated by Student's *t*-test or Mann–Whitney two-sided or ANOVA test, as appropriate, and indicated in each figure legend. Differences were considered significant when $p < 0.05$.

Results

Only LBC displays *CDKN1B* mutations in a relevant number of cases (>1%)

We performed a curated survey of publicly available data banks (i.e. COSMIC and ICGC) to estimate the

presence of *CDKN1B* mutations in different types of cancer. We focused on breast cancer, harboring *CDKN1B* mutations at the highest frequency, and on head and neck and ovarian cancers, with very low frequency mutated models (Table 1). Of note, in this analysis the copy number variation (CNV) and mutations of uncertain significance, such as those in *CDKN1B* introns or causing synonymous substitutions, were not included. This survey confirmed that *CDKN1B* is only mutated in a relevant number of samples (i.e. >1%) in the hormone receptor-positive (HR+) breast cancer subtype (hereafter luminal breast cancer; LBC), as originally reported [7]. Moreover, the analysis of the ICGC data revealed that breast cancer arising in young women (BCYW) displayed more frequent *CDKN1B* alterations. However, this observation arose from the analysis of a small Asian cohort of 50 BCYW, in which one patient was mutated, leading to 2% of observed frequency. Whether BCYW could represent a distinct biological entity from other breast cancers is still a debated matter [34,35]; we therefore considered this possibility worthy of further investigation.

For these reasons, we decided to verify: (1) if *CDKN1B* somatic mutations could be detected at the clonal/subclonal level in breast cancer and, particularly, in the luminal subtype; (2) if *CDKN1B* was more frequently altered in BCYW; (3) if head and neck and ovarian cancer patients may hinder higher frequency of *CDKN1B* mutation when even clonal/subclonal alteration were brought to light; and (4) the reproducibility of detecting clonal/subclonal alteration.

To this aim, we first exploited a custom designed Illumina multi-gene NGS panel and then set up a homemade amplicon-based ultra-deep NGS approach, in which only *CDKN1B* mutations in the coding sequence were annotated. Between January 2016 and December 2019, we collected specimens from breast cancer patients ($n = 396$) at CRO Aviano and at University of Rome 'Sapienza', purposely enriched for LBC ($n = 327$) and BCYW samples ($n = 227$) (Table 2 and supplementary material, Table S1). We also collected liquid biopsies from metastatic breast cancer patients ($n = 62$) at CRO Aviano (supplementary material, Table S2). In addition, we collected specimens from epithelial ovarian cancer patients ($n = 110$), at CRO Aviano between January 2011 and October 2018 (supplementary material, Table S3), and from HNSCC patients ($n = 202$) at CRO Aviano and at General Hospital of Pordenone, between January 2010 and October 2015 (supplementary material, Table S4).

Only one (Q107H) and two (P133T, E126K) mutated samples were identified in epithelial ovarian cancer and HNSCC, respectively, confirming the very low frequency of *CDKN1B* mutations in these tumors (<1%).

With regards to breast cancer, we found 14 mutations (13 somatic and one germinal) in 11 breast cancer patients (Table 3). Mutations found at an allelic frequency (MAF) <10% (11/14) were considered subclonal. However, it is possible that our assumption of subclonality is not correct in all cases, as neoplastic cell content and CNV were precisely assessed for most but not all samples analyzed. Furthermore, 10 somatic mutations, in 10 breast cancer patients, were found using the multi-gene NGS panel but were not annotated, as they could not be confirmed, because either they could not be validated in multiple runs or using different DNA preparation or for unavailability of further DNA (supplementary material, Table S5). Confirmed somatic mutations were all found in LBC patients ($n = 327$; 13 mutations; 10 patients). Together, our large cohort of breast cancer data showed that patients were mutated for *CDKN1B* at 2.8% frequency (11 mutated patients/396 total patients). Considering only the luminal subtype, for which our cohort was however greatly enriched, this percentage increased and reached 3.1% (10 mutated patients – all somatic/327 LBC patients), whereas it dropped to 1.4% when non-luminal breast cancer was considered (triple negative and HER2+; one mutated patient – germinal/69 non-LBC patients).

Interestingly, 10/14 mutations detected were found in tumors from eight young patients. Subdividing LBC patients based on their age (young premenopausal patients <45 years of age, $n = 195$; non-young >45 years of age, $n = 132$), the percentage of mutation increased to 4.1% in the young LBC group (eight mutated patients/195 patients) versus 1.5% in the non-young LBC group (two mutated patients/132 patients). Thus, our data, although not conclusive, suggest an increased frequency of *CDKN1B* mutation in breast cancer arising in premenopausal women.

Table 1. CDKN1B somatic mutation frequency reported in ICGC and COSMIC data portals.

Cancer	Subtypes	ICGC	COSMIC	Total	Percentage
Head and neck		5/1505	8/1452*	13/2957	0.44%
Ovary		0/727	2/1243†	2/1970	0.10%
Breast	All	17/1970	74/4090‡	91/6060	1.50%
	Luminal-HR+	4/569	21/1496‡	25/2065	1.21%
	TNBC/ HER2+	2/257	0/442	2/699	0.29%

Number of CDKN1B somatic mutations of possible clinical significance, as evaluated by curated analyses of ICGC and COSMIC data portals on May 2020. In each column, the number of mutated over total cases analyzed is reported. The final column reports the number and percentage of CDKN1B mutated samples and represents the sum of the cases indicated in the ICGC and COSMIC columns.

Subtypes reports the frequency of CDKN1B in breast cancer cases for which subtype information was available.

*One sample carrying a silent missense mutation (G111=) was also annotated in COSMIC.

†One sample carrying a silent missense mutation (P133=) and one carrying an intronic mutation were also annotated in COSMIC.

‡Nine samples carrying intronic mutations were also annotated in COSMIC.

HR, hormone receptor; HER2, human epidermal growth factor receptor 2; TNBC, triple negative breast cancer.

Table 2. Clinicopathological features of breast cancer patients (n = 396).

Characteristic	n (%)
Age	
Median	44 years
Range	25–94 years
Subtype	
HER2– HR+ Luminal A	107 (27%)
HER2– HR+ Luminal B	220 (56%)
HER2+ HR+	29 (7%)
HER2+ HR-	10 (2%)
TNBC	26 (7%)
Not available or specified	4 (1%)
Tumor grade	
G1	22 (6%)
G2	137 (35%)
G3	215 (54%)
Not available or specified	22 (5%)
Tumor stage	
I	164 (42%)
II	135 (34%)
III	56 (14%)
IV	0 (0%)
Not available or specified	41 (10%)
Nodal status	
N0	190 (48%)
N+	176 (44%)
Not available or specified	30 (8%)
Samples type	
Primary	363 (92%)
Recurrence	12 (3%)
Lymph node metastasis	21 (5%)
Not available or specified	0 (0%)

Luminal A = HR+, Ki-67 < 20%.
Luminal B = HR+, Ki-67 > 20%.
HR, hormone receptor; HER2, human epidermal growth factor receptor 2; TNBC, triple negative breast cancer.

CNV contributes to alter *CDKN1B* in LBC

As p27 is an haploinsufficient oncosuppressor, its allelic loss could be another mechanism exploited for gene inactivation. To rule out this possibility, we next evaluated whether its copy number was maintained stably diploid in tumors (Table 4). Using ddPCR, we analyzed *CDKN1B* CNV in 187 mammary tumors (139 HR+ LBC, 19 HER2+ HR+, 8 HER2+ HR– and 21 triple negative) from the previous cohort. The results showed that 11.8% of the analyzed breast cancer patients displayed a *CDKN1B* CNV, with 7.5% having a loss (14/187 patients) and 4.3% a gain (8/187 patients). Interestingly, when only LBC were considered, the percentage of CNV raised to 13.7% (19/139 LBC patients) compared with 6.2% found in breast cancer patients of all other subtypes (3/48 patients), again indicating that *CDKN1B* is mainly altered in the luminal subtype. The analysis of LBC patients based on their age, showed a clear difference in the ratio between CNV for *CDKN1B* loss or gain: young LBC patients displayed a loss of *CDKN1B* in 12% of cases (6/50 young LBC patients) and a gain in only 2% (1/50 young LBC patients). On the other side, non-young LBC patients presented an equal rate of *CDKN1B* loss (7%, 6/89 non-young LBC patients) and gain (8%, 7/89 non-young LBC patients). These findings support the possibility that loss of p27, via either protein mutation, truncation or allelic CNV, could represent a significant event in the onset and progression of LBC of premenopausal women.

To verify if altered CNV had any consequence on p27 protein expression and localization, we performed immunohistochemistry for p27 on eight tumor samples with known CNV (five with copy number loss and three with copy number gain). In the tumor, p27 was almost invariably expressed both in the nucleus and in the cytoplasm, whereas in normal mammary ducts, adjacent to the tumor, p27 was strongly nuclear (supplementary material, Figure S1A; see left panels of BC #25 and BC #22). As expected, a different copy number corresponded to a different protein expression, with a strong direct correlation (r = 0.76) (supplementary material, Figure S1B). We also performed the immunohistochemistry analysis on seven mutated tumors; however, given that p27 mutations are mostly below MAF 10% and that the antibody may fail to recognize the mutated protein (especially when truncated), it was not possible to establish any clear connection between the type of mutation and the expression and localization of p27. Only the case of BC #257, mutated P69L at ~30% is reported, showing

Table 3. MAF of *CDKN1B* in breast cancer patients (n = 396).

ID #	Age (years)	Histotype	Subtype	Stage	Protein position	MAF
#351	29	Ductal	Luminal A	IIIA	A121V	27%
#242	40	Ductal	Luminal A	IB	P91H	8.9%
#243	40	Ductal	Luminal A	IC	E22*; P95S	5.5%; 3.7%
#257	40	Lobular	Luminal B	IA	P69L	29.8%
#235	41	Ductal	Luminal B	IC	A98S	7.3%
#190	42	Ductal	Luminal A	IIA	Q57P fs*15	7.6%
#225	44	Ductal	Luminal B	IC	R196H	2.3%
#226	44	Ductal	Luminal B	IC	R15W; C49*	7.4%; 4.7%
#170	47	NA	Triple negative	IIA	I119T	34%
#62	55	Ductal	Luminal B	IA	Y74*	2.8%
#377	72	Ductal	Luminal B	IIA	S27*; Q65E	5.7%; 4.1%

Patients (ID#) have been ordered by their age (increasing).
Luminal A = HR+, Ki-67 < 20%.
Luminal B = HR+, Ki-67 > 20%.
NA, not available.

Table 4. CNV of *CDKN1B* in breast cancer patients (n = 187).

ID #	Age (years)	Histotype	Subtype	CNV
#22	37	Ductal	HER2+ HR–	
#8	38	Ductal	Luminal B	
#32	40	Ductal	Luminal A	
#17	40	Ductal	Luminal B	
#68	42	Ductal	Luminal B	
#169	45	Ductal	Luminal B	
#104	49	Ductal	Luminal B	
#62	55	Ductal	Luminal B	
#183	61	Ductal	Luminal A	
#25	61	Ductal	HER2+ HR+	
#181	64	Ductal	Luminal A	
#3	73	NA	Luminal A	
#82	78	Ductal	Triple negative	
#86	86	Lobular	Luminal B	
#18	31	Ductal	Luminal B	
#127	48	Ductal	Luminal B	
#28	57	Ductal	Luminal B	
#34	65	Ductal	Luminal B	
#38	68	Lobular	Luminal B	
#163	75	Ductal	Luminal A	
#146	75	Ductal	Luminal A	
#63	78	Lobular	Luminal A	

Patients (ID#) have been ordered by their age (increasing) within two main groups: loss (green) or gain (orange) of *CDKN1B*.
Pink colored cells in the table indicate patients <45 years of age.
Luminal A = HR+, Ki-67 < 20%.
Luminal B = HR+, Ki-67 > 20%.
HR, hormone receptor; HER2, human epidermal growth factor receptor 2; NA, not available.

that the tumor displays areas completely negative for p27 and the expression is overall lower and more cytoplasmic than in the normal mammary ducts (supplementary material, Figure S1A, upper panels).

To verify whether *CDKN1B* could be related to progression more than to onset of LBC, we next used a cohort of 62 metastatic patients, 59 of whom had LBC, to evaluate the presence of *CDKN1B* mutations in ccfDNA (Table 5). These patients displayed a substantially higher mutation frequency (8.5%, five mutations/59 metastatic LBC patients, four somatic and one germinal), suggesting that *CDKN1B* alterations may more frequently occur later during the disease progression, as recently observed by others [13], and/or they could be selected under therapeutic pressure. Furthermore, looking at the age of these patients, we could observe that three of five mutated patients were of young age (3/25 young patients, 12%), whereas two were non-young (2/34 non-young patients, 5.9%). Next, we carried out an analysis to establish whether a correlation may exist between the presence of CDKN1B alteration and clinical parameters, such as relapse and survival. Data collected on this small cohort of metastatic LBC patients clearly indicate that CDKN1B mutational status significantly impacts on progression-free survival (n = 59, five mutated; supplementary material, Figure S2A). The progression-free survival curves were even more different when only metastatic LBC patients treated with endocrine therapies were analyzed (n = 47, four mutated; supplementary material, Figure S2B).

Expression of *CDKN1B* C-terminal deletion mutants does not rescue p27 functions in LBC cells

Of the 13 somatic mutations (Figure 1A, see long lines) that we identified in LBC solid biopsies, four generated a stop codon and resulted in the loss of p27 C-terminus. This observation confirmed the higher frequency of truncating/frame shift mutations among the different mutations that were observed in sporadic breast cancer [7,8] (Figure 1A, see short lines) and supported the possibility that truncation of p27 C-terminus directly contributes to onset and/or progression of breast cancer, as we and others have recently proposed [12,28,36–38].

To verify this hypothesis, we moved to an *in vitro* model of LBC and exploited the LBC cell line MCF-7, in which we recently generated KO of the *CDKN1B* gene [28]. In these p27KO MCF-7 cells, we KI two p27 truncated mutants, namely p27 K134fs*11 ($p27^{K134fs}$) and the p27 T171* ($p27^{T171*}$), previously identified in patients with LBC by the group of Ellis [8] (see short lines written in red, in Figure 1A). The $p27^{T171*}$ mutant carries a nonsense mutation at codon 171 resulting in loss of the last 28 amino acids, a region representing the so-called intrinsically disordered region of p27, known to be involved in many protein interactions and containing many phosphorylation sites [12]. The $p27^{K134fs}$ mutant loses the intrinsically disordered region and also the nuclear localization signal (amino acids 152–168). The sequence of p27 WT ($p27^{WT}$) was also reintroduced, to generate KI 'rescue' clones, as control. The WT and the two p27 mutants were KI into the adeno-associated virus integration site 1 (AAVS1), located in human chromosome 19 and considered a safe harbor locus for transgene integration. Re-expression of exogenous p27 in this locus resulted in comparable copies of the endogenous one, allowing us to better evaluate the real biological effects of these mutants (supplementary material, Figure S3A,B). At the protein level, the $p27^{T171*}$ mutant was more expressed than $p27^{WT}$, in line with the fact that $p27^{T171*}$ lacks the phosphorylation sites

Table 5. MAF of *CDKN1B* in liquid biopsies from metastatic breast cancer patients (n = 62).

ID #	Age (years)	Histotype	Subtype	Stage	Protein position	MAF
LB#3	36	Ductal	Luminal	IV	I119T	52%
LB#15	38	Ductal	Luminal	IV	P35Q	4.4%
LB#10	44	Lobular	Luminal	IV	E46 *; W60*	16%; 37%
LB#60	55	Lobular	Luminal	IV	G34C	1.5%
LB#67	54	Ductal	Luminal	IV	K96E	36%

Patients (ID#) ordered by their age (increasing).

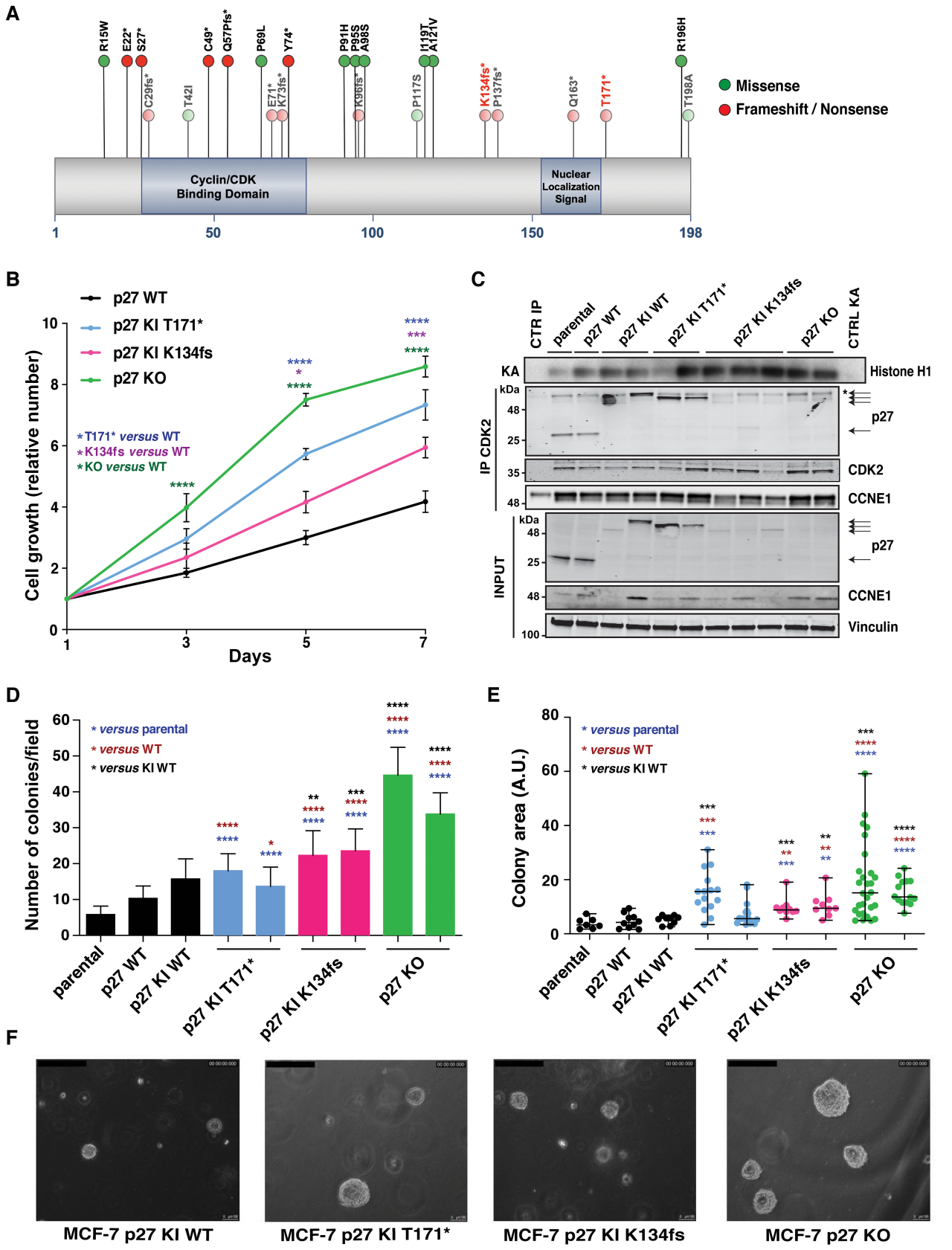

Figure 1 Legend on next page.

T187 and T198, both controlling p27 protein stability (supplementary material, Figure S3C). On the opposite, the $p27^{K134fs}$ mutant was less expressed than $p27^{WT}$, suggesting that this truncated p27 mutant was less stable, a hypothesis confirmed by a time course treatment with cycloheximide (supplementary material, Figure S3C–E).

First, we analyzed the proliferation of these clones and evaluated the impact of the expression of these mutants in the context of p27KO MCF-7 cells. The analysis of cell proliferation under normal cell culture conditions showed that, as expected, p27KO MCF-7 cells displayed a significant proliferative advantage and that $p27^{T171*}$ and $p27^{K134fs}$ KI clones proliferated at an intermediate level, between parental and p27KO clones, probably indicating that the presence of the CDK-binding domain in the N-terminal portion of both KI mutants was still able to partially restrain cell cycle progression (Figure 1B). These data were confirmed by FACS analyses of DNA content, showing that p27KO cells were less sensitive to serum starvation and re-entered the cell cycle faster than MCF-7 cells expressing the $p27^{WT}$ and cells expressing $p27^{T171*}$ and the $p27^{K134fs}$ displayed an intermediate behavior (supplementary material, Figure S4A). Further confirmation was obtained by kinase assay, evaluating the activity of CDK2 and showing that the two mutants, although able to bind CDK2, were less efficient in inhibiting its kinase activity (Figure 1C). To explain this phenotype, we also looked at the cytonuclear distribution of these mutants and observed that the mutant K134fs was not only expressed at a very low level, but was almost exclusively cytoplasmic, as expected by the fact that it has lost its nuclear localization signal (supplementary material, Figure S4B). On the other hand, the T171* mutant, similarly to the WT protein, was expressed both in nuclear and cytoplasmic compartments, with a prevalence in the nuclear fraction (supplementary material, Figure S4B). This evidence is in line with the notion that phosphorylation of the T187 is necessary for p27 protein nuclear degradation and that the T171* mutant lacks this residue.

We then moved to the analysis of anchorage-independent cell growth, a parameter that well correlates with tumorigenicity. Loss of p27 strongly increased the ability of MCF-7 cells to grow under this condition, both in terms of colony number and colony area (Figure 1D, E) and the same was true using another LBC cell line, the T47D stably silenced for p27 (supplementary material, Figure S5). Notably, these phenotypes were rescued by the $p27^{WT}$ KI but only partially by the $p27^{T171*}$ and $p27^{K134fs}$ KI. The mutants behaved more similarly to the p27WT considering the colony area, but more similarly to the p27KO cells considering the colony number, suggesting that these two aspects may be controlled by different p27 domains and activities (Figure 1D,E).

We next tested if p27 absence and/or deletion of its C-terminus had an impact on the ability to grow and establish cell polarity when cells were cultured in 3D matrices. To this aim, MCF-7 cells were cultured in 3D-Matrigel and colonies were counted and immunostained, to evaluate their growth and morphology. In line with the above results, the absence of p27 or the expression of the mutants resulted in a higher number of colonies that were also more proliferative, as demonstrated by an increased number of Ki-67-positive cells (Figure 2A,B). Interestingly, whereas cells expressing the WT protein formed well-shaped, acini-like structures, p27KO cells and those expressing the $p27^{T171*}$ and $p27^{K134fs}$ mutants formed highly disorganized structures, in which the apical-basal polarity of the acinus was completely disrupted (Figure 2C). These data were confirmed in T47D stably silenced for p27 and grown in 3D-Matrigel (supplementary material, Figure S6).

Discussion

In this work we assessed the frequency of *CDKN1B* mutations in a large cohort of cancer patients and observed that *CDKN1B* mutations are more frequent in LBC than in other breast cancer subtypes or other types of cancer analyzed (i.e. HNSCC and epithelial ovarian cancer). Our data do not support the observation previously made in SI-NET [2] that suggested the use of deeper sequencing approaches to significantly increase the identification of *CDKN1B* mutated subclones. Yet, based on the results obtained in ccfDNA from metastatic patients (8.5%), we hypothesize that assessing *CDKN1B* status during disease progression and following it over time, could better show the contribution of p27 to breast cancer, as also recently proposed by others [13]. Studies with larger numbers of samples will be necessary to confirm this hypothesis.

Many subclonal mutations we found with multi-gene panels were not confirmed using a deeper and targeted sequencing approach. This observation suggests that caution should be taken when large-scale sequencing approaches are used to identify subclonal mutations in

Figure 1. Loss of *CDKN1B* and expression of C-terminal deletion mutants alter the growth of LBC cells. (A) Lollipop representation of CDKN1B mutations, identified in our cohort of solid biopsies (long lines, bright colors) or by others [7,8] (short lines, faded colors). The length of the lines does not indicate the mutation frequency: each of all mutations has only been retrieved in one sample. Green dots indicate missense mutations and red dots indicate frameshift/nonsense mutations. The two mutations chosen for the functional studies in MCF-7 cells (K134fs* and E171*), identified by Ellis *et al* [8], are written in red. (B) Data from growth curve analysis of MCF-7 p27-modified cell clones, expressed as fold-increase over the number of cells plated on day 1. ANOVA test has been used for statistical analysis. (C) Kinase assay and western blot analysis of co-immunoprecipitated cyclin E-CDK2 complex. Upper panel shows *in vitro* phosphorylation assay, using histone H1 as substrate. Arrows mark p27 at different molecular weights, from top: KI $p27^{WT}$, KI $p27^{T171*}$, KI $p27^{K134fs}$, and endogenous p27. Asterisk marks a non-specific band in the immunoprecipitate. (D,E) Number of colonies (D) and area (E) of MCF-7 p27-modified clones grown in soft agar for 2 weeks. Colony size was measured using Image Lab™ software. Mann–Whitney test and Student's *t*-test have been used for statistical analysis, as more appropriate. (F) Representative bright field images of the colonies from the experiment described in (D) and (E). 10× magnifications are shown. Asterisks indicate significant differences, $*p \le 0.05$; $**p \le 0.01$; $***p \le 0.001$; $****$ $p \le 0.0001$.

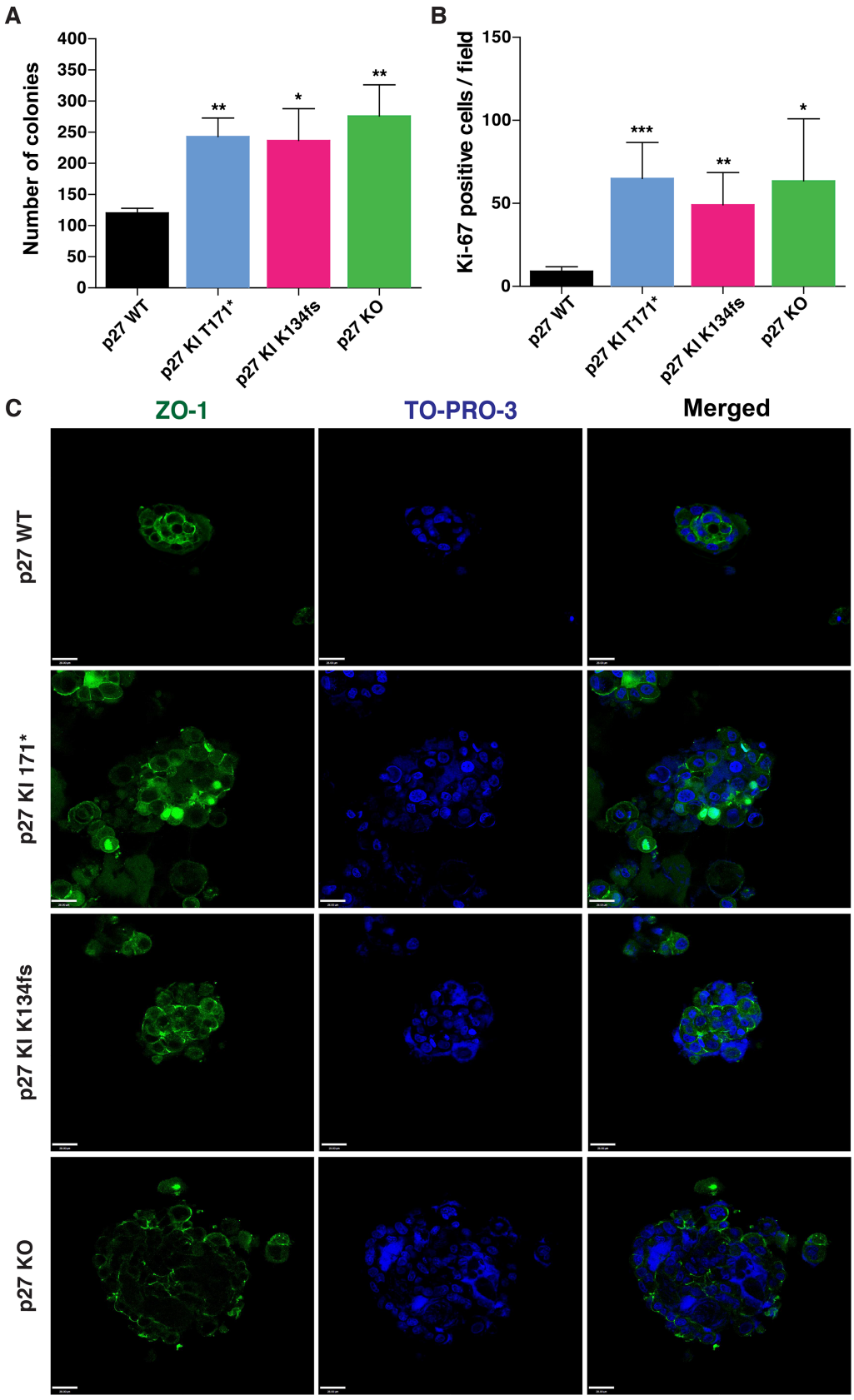

Figure 2. Loss of *CDKN1B* and expression of C-terminal deletion mutants alter the growth and polarity of LBC cells in 3D-Matrigel. (A) Number of mammary acini of MCF-7 p27-modified clones included in 3D-Matrigel and grown in DMEM 0.1% FBS medium supplemented with 3% of wound fluid. (B) Quantification of immunofluorescence staining for Ki-67 in mammary acini from the experiment described in (A). For each clone, Ki-67-positive cells were counted in four fields and the results normalized to the area of the colony, measured using ImageJ software. (C) Representative confocal images of immunofluorescence analyses of mammary acini of the experiment described in (A). Acini were immunostained for ZO-1 (green, left panels) and nuclei detected using TO-PRO-3 (blue, central panels). Green intracytoplasmic signal in KI clones is due to GFP-p27 mutant expression. Scale bar, 28 μm. Student's *t*-test was used for statistical analysis. Asterisks indicate significant differences, $*p \leq 0.05$; $**p \leq 0.01$; $***p \leq 0.001$.

human cancer. A limitation of our study is that some of the mutations were found in FFPE samples at low MAF but we did not have the possibility to test them with an orthogonal technique. This technical aspect will certainly need to be implemented if FFPE samples are chosen in the future for this type of characterization. Furthermore, as we limited our sequencing approach to the coding region of p27, there is still the possibility that we missed other mutations potentially affecting p27 expression by altering the promoter or 5'- or 3'-UTR regions.

From our analyses, we confirm literature data indicating that *CDKN1B* is mutated predominantly in LBC (3.1%) and our data also suggest an increased mutation rate in young women with LBC (4.1%), as previously reported in a small Asian cohort of breast cancer samples from ICGC datasets. However, given the overall low frequency of *CDKN1B* mutations, more abundant cohorts of BCYW need to be collected and analyzed before drawing a definitive conclusion. The data collected from the CNV also support the same observation (12%), overall strengthening the possibility that breast cancer arising in premenopausal women more frequently lose p27 expression or activity to initiate and/or progress. This possibility is indirectly sustained by literature data showing that p27 expression in normal breast tissue may be used as a read out of the fraction of actively cycling cells and this, in turn, may represent a marker for breast cancer risk assessment in premenopausal women [37]. Furthermore, it is well accepted that mammary epithelial progenitors are the normal cell-of-origin of breast cancer and it has been clearly shown in animal models that p27 regulates the number of hormone-responsive luminal progenitors that eventually impact on breast cancer risk [38]. In another study, the human normal mammary gland was profiled and a subset of p27+ cells that might represent quiescent hormone-responsive progenitors was identified [39]. A significant reduction in the frequency of these p27+ progenitor cells was observed in parous versus non-parous and BRCA1/2 mutated women, suggesting that pathways controlling the number of these p27+ cells directly related to breast cancer risk and could be explored for cancer risk assessment and prevention [39]. Consistent with this, p27 deficiency in mice was associated with hypoplasia, impaired ductal branching and lobulo-alveolar differentiation [40], a phenotype consistent with a putative role for p27 in regulating the number and proliferation of mammary epithelial progenitors. Of note, we and others have observed that an absence of p27 in *Cdkn1b*$^{-/-}$ female animals induces dramatic changes in mammary epithelial cells, probably due to altered hormonal signaling and perturbed endocrine environment [38] (G Mungo, personal communication October 2020).

Finally, we highlight that, compared with germline mutations, somatic p27 alterations more frequently result in the formation of truncated, frameshifted proteins. Using a highly controlled *in vitro* model, we report that, unlike the p27 WT, the p27 truncated mutants are essentially unable to revert the pro-tumorigenic program set up by the loss of p27 gene in MCF-7 cells.

Taken together, by combining a genomic analysis on a large number of human cancers and a highly controlled *in vitro* approach, we have established a central role for p27 in LBC. Although the overall rate of mutated LBC remains quite low, we highlight here that alterations can also be found as CNV alteration and our findings, together with the notion that p27 is also frequently degraded and/or delocalized from the nucleus in these tumors, support a central role for p27 in the control of hormone-dependent breast cancer, as previously suggested [7,8,12,15]. For a clinical application of our findings, it would be crucial to identify which, if any, subsets of patients are enriched for p27 abnormalities. Otherwise, their overall low frequency, when looked across all breast cancer, may preclude a relevant role for p27 in the clinical setting. In this regard, a small increase in the lobular versus ductal histotype was noticed among the patients carrying p27 alteration; however, a larger number of patients with this histotype will need to be screened to find a statistical significance. In the relatively small number of samples that we could test, no correlation with *BRCA1/2* or *PIK3CA* mutational status was observed (not shown).

Moreover, analyzing multiple tumor biopsies from the same patient or following-up patients with liquid biopsies during disease evolution, as we are currently pursuing, will be important to dissect whether breast cancer subclones carrying *CDKN1B* mutation are enriched in those patients that experience progressive disease. Our data on metastatic LBC patients suggest that p27 mutational status could be used as a biomarker to identify more aggressive LBC that might need closer follow-up or specific targeted treatments, but larger cohorts of breast cancer samples will be needed to validate this possibility.

In conclusion, by combining genomic analyses of human samples with *in vitro* validation mechanistic studies, our work establishes a central role for p27 in the progression of LBC and also highlights the relevance of its C-terminus in the control of breast cancer cell growth.

Acknowledgements

We are grateful to the patients who consented to donating their samples. We also thank all present and past members of the SCICC laboratory for their valuable contributions; all members of the Molecular Oncology Unit for critical discussion of the data; the Pathology Unit staff for their valuable technical support; and the CRO Institutional Biobank for their excellent support. This work was supported by the Associazione Italiana per la Ricerca sul Cancro (AIRC) to B Belletti (AIRC IG# 20061) and to G Baldassarre (AIRC IG# 16865); by CRO Intramural Research Grant (5X1000_2016_MdS) to I Segatto; by L.R. 17/2014-Regione FVG (TNBCneo and PERMID) to G Baldassarre; by Ministero della Salute (RF-2016-02361041) to M Sonego; by the CRO Ricerca Corrente core grant (linea 1) of Ministero della Salute; by Associazione Italiana per la Ricerca sul Cancro (AIRC

fellowships) to I Segatto (AIRC fellowship #18171) and F Citron (AIRC fellowship #20902).

Author contributions statement

DV and FR contributed equally to this work. BB and GB conceived, designed and supervised the overall study. DV, FR, IA, IS, GLRV, ADA, MC, SDA, FC, LM, MCM and GM carried out experiments. RB, TP, MS, LG, FV, MSN, MS, SM, RS, LB, GF, GG, EL, SS, VG, JP, FT, VC, FP, VG and AV provided expertise and collected clinical samples and data. DV, FR, BB and GB performed statistical analyses and generated figures and tables. BB and GB wrote the manuscript. All authors contributed to this work and reviewed and approved the final manuscript.

Data availability statement

The NGS data have been deposited with the SRA of NCBI, under the access number PRJNA660629.

References

1. Barbieri CE, Baca SC, Lawrence MS, *et al*. Exome sequencing identifies recurrent SPOP, FOXA1 and MED12 mutations in prostate cancer. *Nat Genet* 2012; **44:** 685–689.
2. Francis JM, Kiezun A, Ramos AH, *et al*. Somatic mutation of CDKN1B in small intestine neuroendocrine tumors. *Nat Genet* 2013; **45:** 1483–1486.
3. Lee M, Pellegata NS. Multiple endocrine neoplasia type 4. *Front Horm Res* 2013; **41:** 63–78.
4. Fero ML, Rivkin M, Tasch M, *et al*. A syndrome of multiorgan hyperplasia with features of gigantism, tumorigenesis, and female sterility in p27(Kip1)-deficient mice. *Cell* 1996; **85:** 733–744.
5. Fero ML, Randel E, Gurley KE, *et al*. The murine gene p27Kip1 is haplo-insufficient for tumour suppression. *Nature* 1998; **396:** 177–180.
6. Cancer Genome Atlas Network. Comprehensive molecular portraits of human breast tumours. *Nature* 2012; **490:** 61–70.
7. Stephens PJ, Tarpey PS, Davies H, *et al*. The landscape of cancer genes and mutational processes in breast cancer. *Nature* 2012; **486:** 400–404.
8. Ellis MJ, Ding L, Shen D, *et al*. Whole-genome analysis informs breast cancer response to aromatase inhibition. *Nature* 2012; **486:** 353–360.
9. Liu Y, Hu Z. Identification of collaborative driver pathways in breast cancer. *BMC Genomics* 2014; **15:** 605.
10. Spirin KS, Simpson JF, Takeuchi S, *et al*. p27/Kip1 mutation found in breast cancer. *Cancer Res* 1996; **56:** 2400–2404.
11. Tigli H, Buyru N, Dalay N. Molecular analysis of the P27/Kip1 gene in breast cancer. *Mol Diagn* 2005; **9:** 17–21.
12. Cusan M, Mungo G, De Marco Zompit M, *et al*. Landscape of CDKN1B mutations in luminal breast cancer and other hormone-driven human tumors. *Front Endocrinol (Lausanne)* 2018; **9:** 393.
13. Rinaldi J, Sokol ES, Hartmaier RJ, *et al*. The genomic landscape of metastatic breast cancer: insights from 11,000 tumors. *PLoS One* 2020; **15:** e0231999.
14. Pohl G, Rudas M, Dietze O, *et al*. High p27Kip1 expression predicts superior relapse-free and overall survival for premenopausal women with early-stage breast cancer receiving adjuvant treatment with tamoxifen plus goserelin. *J Clin Oncol* 2003; **21:** 3594–3600.
15. Stendahl M, Nilsson S, Wigerup C, *et al*. p27Kip1 is a predictive factor for tamoxifen treatment response but not a prognostic marker in premenopausal breast cancer patients. *Int J Cancer* 2010; **127:** 2851–2858.
16. Payne SR, Zhang S, Tsuchiya K, *et al*. p27kip1 deficiency impairs G2/M arrest in response to DNA damage, leading to an increase in genetic instability. *Mol Cell Biol* 2008; **28:** 258–268.
17. Nahta R, Takahashi T, Ueno NT, *et al*. P27(kip1) down-regulation is associated with trastuzumab resistance in breast cancer cells. *Cancer Res* 2004; **64:** 3981–3986.
18. Lee-Hoeflich ST, Pham TQ, Dowbenko D, *et al*. PPM1H is a p27 phosphatase implicated in trastuzumab resistance. *Cancer Discov* 2011; **1:** 326–337.
19. Zhao H, Faltermeier CM, Mendelsohn L, *et al*. Mislocalization of p27 to the cytoplasm of breast cancer cells confers resistance to anti-HER2 targeted therapy. *Oncotarget* 2014; **5:** 12704–12714.
20. Guiley KZ, Stevenson JW, Lou K, *et al*. p27 allosterically activates cyclin-dependent kinase 4 and antagonizes palbociclib inhibition. *Science* 2019; **366:** eaaw2106.
21. Vilgelm AE, Saleh N, Shattuck-Brandt R, *et al*. MDM2 antagonists overcome intrinsic resistance to CDK4/6 inhibition by inducing p21. *Sci Transl Med* 2019; **11:** eaav7171.
22. American Joint Committee on Cancer. In *AJCC Cancer Staging Manual* (8th edn), Amin MB, Greene FL, Edge SB (eds). Springer: New York, 2017.
23. Wolff AC, Hammond MEH, Allison KH, *et al*. Human epidermal growth factor receptor 2 testing in breast cancer: American Society of Clinical Oncology/College of American Pathologists Clinical Practice Guideline Focused Update. *J Clin Oncol* 2018; **36:** 2105–2122.
24. World Health Organization. *World Health Statistics 2019: Monitoring Health for the SDGs : Sustainable Development Goals*. World Health Organization: Geneva, 2019.
25. World Health Organization. *World Health Statistics 2017: Monitoring Health for the SDGs, Sustainable Development Goals*. World Health Organization: Geneva, 2017.
26. Thorvaldsdottir H, Robinson JT, Mesirov JP. Integrative Genomics Viewer (IGV): high-performance genomics data visualization and exploration. *Brief Bioinform* 2013; **14:** 178–192.
27. Smigielski EM, Sirotkin K, Ward M, *et al*. dbSNP: a database of single nucleotide polymorphisms. *Nucleic Acids Res* 2000; **28:** 352–355.
28. Berton S, Cusan M, Segatto I, *et al*. Loss of p27kip1 increases genomic instability and induces radio-resistance in luminal breast cancer cells. *Sci Rep* 2017; **7:** 595.
29. Berton S, Pellizzari I, Fabris L, *et al*. Genetic characterization of p27 (kip1) and stathmin in controlling cell proliferation in vivo. *Cell Cycle* 2014; **13:** 3100–3111.
30. Segatto I, Zompit MDM, Citron F, *et al*. Stathmin is required for normal mouse mammary gland development and Δ16HER2-driven tumorigenesis. *Cancer Res* 2019; **79:** 397–409.
31. Belletti B, Vaidya JS, D'Andrea S, *et al*. Targeted intraoperative radiotherapy impairs the stimulation of breast cancer cell proliferation and invasion caused by surgical wounding. *Clin Cancer Res* 2008; **14:** 1325–1332.
32. Citron F, Segatto I, Vinciguerra GLR, *et al*. Downregulation of miR-223 expression is an early event during mammary transformation and confers resistance to CDK4/6 inhibitors in luminal breast cancer. *Cancer Res* 2020; **80:** 1064–1077.
33. Fabris L, Berton S, Citron F, *et al*. Radiotherapy-induced miR-223 prevents relapse of breast cancer by targeting the EGF pathway. *Oncogene* 2016; **35:** 4914–4926.
34. Azim HA, Partridge AH. Biology of breast cancer in young women. *Breast Cancer Res* 2014; **16:** 427.

35. Partridge AH, Pagani O, Abulkhair O, *et al*. First international consensus guidelines for breast cancer in young women (BCY1). *Breast* 2014; **23:** 209–220.
36. Rampioni Vinciguerra GL, Citron F, Segatto I, *et al*. p27kip1 at the crossroad between actin and microtubule dynamics. *Cell Division* 2019; **14:** 2.
37. Huh SJ, Oh H, Peterson MA, *et al*. The proliferative activity of mammary epithelial cells in normal tissue predicts breast cancer risk in premenopausal women. *Cancer Res* 2016; **76:** 1926–1934.
38. Ding L, Shunkwiler LB, Harper NW, *et al*. Deletion of Cdkn1b in ACI rats leads to increased proliferation and pregnancy-associated changes in the mammary gland due to perturbed systemic endocrine environment. *PLoS Genet* 2019; **15:** e1008002.
39. Choudhury S, Almendro V, Merino VF, *et al*. Molecular profiling of human mammary gland links breast cancer risk to a p27+ cell population with progenitor characteristics. *Cell Stem Cell* 2013; **13:** 117–130.
40. Muraoka RS, Lenferink AE, Simpson J, *et al*. Cyclin-dependent kinase inhibitor p27(Kip1) is required for mouse mammary gland morphogenesis and function. *J Cell Biol* 2001; **153:** 917–932.

SUPPLEMENTARY MATERIAL ONLINE

Supplementary materials and methods

Figure S1. p27 protein expression correlates with CDKN1B copy number in breast cancer samples

Figure S2. p27 mutations in liquid biopsies of metastatic breast cancer patients correlates with worse progression-free survival

Figure S3. *CDKN1B* truncation mutants display altered protein stability compared with the WT form

Figure S4. Loss of *CDKN1B* and expression of C-terminal deletion mutants alter S-phase entry and cytonuclear localization in LBC cells

Figure S5. Silencing of p27 induces increased anchorage independent growth in LBC cells

Figure S6. Loss of CDKN1B alters the growth of LBC cells in 3D-Matrigel

Table S1. Clinicopathological features of young (<45 years old) premenopausal breast cancer patients (n = 227)

Table S2. Clinicopathological features of breast cancer patients analyzed by liquid biopsy (n = 62)

Table S3. Clinicopathological features of ovarian cancer patients (n = 110)

Table S4. Clinicopathological features of head and neck cancer patients (n = 202)

Table S5. Mutations of *CDKN1B* detected by multi-gene panel and not confirmed by targeted sequencing in breast cancer patients